

Journal of Materials Chemistry A

Materials for energy and sustainability

Accepted Manuscript

This article can be cited before page numbers have been issued, to do this please use: J. Kaur, G. Asadiankouhidehkordi, V. Singh, A. C. Liberati, A. Diraki, S. Bendahmane, M. D. Aloisio, P. Patel, J. Henderson, F. B. Ettouil, C. Crudden, M. C. Biesinger, A. Levasseur, C. Moreau and J. Mauzeroll, *J. Mater. Chem. A*, 2025, DOI: 10.1039/D4TA07631A.



This is an Accepted Manuscript, which has been through the Royal Society of Chemistry peer review process and has been accepted for publication.

Accepted Manuscripts are published online shortly after acceptance, before technical editing, formatting and proof reading. Using this free service, authors can make their results available to the community, in citable form, before we publish the edited article. We will replace this Accepted Manuscript with the edited and formatted Advance Article as soon as it is available.

You can find more information about Accepted Manuscripts in the [Information for Authors](#).

Please note that technical editing may introduce minor changes to the text and/or graphics, which may alter content. The journal's standard [Terms & Conditions](#) and the [Ethical guidelines](#) still apply. In no event shall the Royal Society of Chemistry be held responsible for any errors or omissions in this Accepted Manuscript or any consequences arising from the use of any information it contains.

ARTICLE

N-heterocyclic Carbene-Promoted Copper Powder Conditioning for Thermal Spray Applications

Jashanpreet Kaur^{‡a,f}, Golnoush Asadiankouhidehkordi^{‡b,f}, Vikram Singh^{a,f}, Andre C. Liberati^{b,f}, Ahmad Diraki^{c,f}, Souhaila Bendahmane^{c,f}, Mark D. Aloisio^{d,f}, Payank Patel^{b,f}, Jeffrey Henderson^e, Fadhel Ben Ettouil^b, Cathleen M. Crudden^{*d,f}, Mark Biesinger^{*e,f}, Annie Levasseur^{*c,f}, Christian Moreau^{*b,f}, Janine Mauzeroll^{*a,f}

Received 00th January 20xx,
Accepted 00th January 20xx

DOI: 10.1039/x0xx00000x

Copper powder is essential in the thermal spray industry for its excellent thermal and electrical conductivity. However, uncontrolled surface oxide on Cu powder degrades coating performance by weakening inter-particle bonding. This study introduces a novel method using N-heterocyclic carbene (NHC) chemistry to remove surface oxides from Cu powder via a one-pot immersion process. NHC functionalization not only eliminates surface oxides but also acts as a capping agent, enhancing the corrosion resistance of the sprayed coatings. Detailed investigations using scanning electron microscopy, X-ray photoelectron spectroscopy, and laser desorption/ionization spectroscopy confirmed the successful NHC treatment. The process was scaled up from gram to kilogram scale, demonstrating its industrial feasibility. Mechanical and corrosion tests show that NHC-treated Cu powder thermal sprayed coatings have superior inter-particle bonding compared to those from untreated-Cu powder. This approach shows great promise for improving the quality of metal powder coatings by effectively removing surface oxides.

Introduction

Thermal spraying comprises a family of industrial coating processes applied to a broad range of components¹ to enhance their surface properties in aerospace, automotive, oil and gas, biomedical, manufacturing, etc.²⁻⁴ The use of high-velocity air-fuel (HVOF) process or other spray processes to deposit Cu particles^{2,5-8} has yet to reach its full industrial potential because oxide forms on the surface under ambient conditions in an uncontrolled manner, which is known to increase with storage time⁹ and under different spray conditions.¹⁰

Generally, in the thermal spraying processes, powder particles injected into the flame are heated to a semi-molten state and accelerated to high velocities before they impinge on the

substrate.^{2,7,11} Upon impact, they undergo plastic deformation, flattening, and bonding to the substrate, and dense coatings are produced with remarkable adherence and minimal thermal degradation.^{2,8} In general, metals or alloys form bonds when the fresh metal surface of one particle comes in contact with that of another.¹² In particular, in the HVOF process in which solid particles are sprayed at high speed, the oxide layer on powder particles diminishes the plastic deformation upon impact. This is problematic because different powder oxide thicknesses influence the quality of bonding in the final coating.^{5,13,14}

Oxide presence reduces the adhesion with the substrate and cohesion amongst the sprayed particles, which decreases the deposition efficiency of Cu powder and can lead to the deterioration of the thermal and electrical conductivity of the final coating.^{15,16} Thus, the development of new surface chemistry to remove copper surface oxide is key to improving the performance of Cu-sprayed coatings. This negative influence of an oxide layer on the surface of the spray particles is present in spraying several other types of metals and alloys.

The removal of copper oxides from planar or particulate surfaces has been studied through H₂ gas treatment¹⁷, D* and CH₃* radicals¹⁸, vacuum annealing of coated films¹⁹ or powders,^{16,20} glacial acetic acid treatment²¹ and acid pickling.²² While these methods can remove oxide, they lack the ability to cap the surface and prevent further oxidation. Additionally, any methods requiring ultra-high vacuum conditions are untenable for thermal spray applications.

‡ Equally Contributing Authors

* Corresponding Authors

^a Department of Chemistry, McGill University, Montréal, Québec, H3A 0C7, Canada.

Email: janine.mauzeroll@mcgill.ca

^b Department of Mechanical, Industrial and Aerospace Engineering, Concordia University Montreal, Quebec, H3G 1M8, Canada.

Email: christian.moreau@concordia.ca

^c Département de génie de la construction, École de technologie supérieure, Montréal, Québec, H3C 1K3, Canada

Email: annie.levasseur@etsmtl.ca

^d Department of Chemistry, Queen's University, Kingston, Ontario K7L 3N6, Canada.

Email: cruddenc@chem.queensu.ca

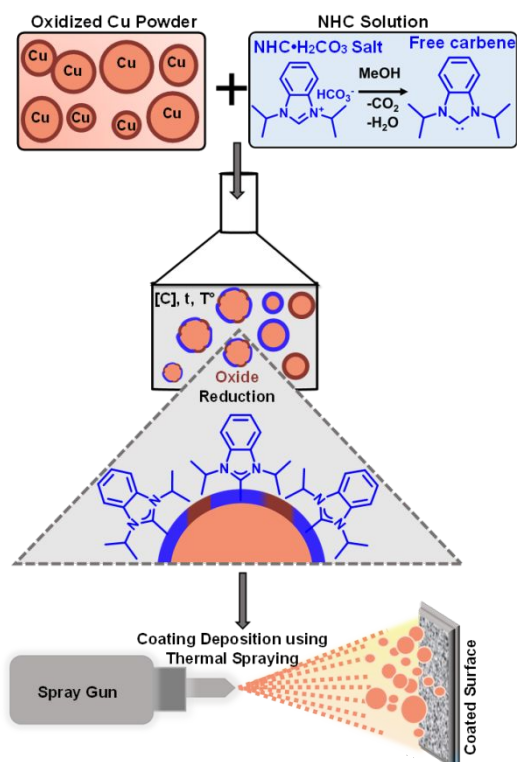
^e Surface Science Western, Western University, 999 Collip Circle, Suite LL31, London, Ontario, N6G 0J3, Canada.

Email: biesingr@uwo.ca

^f Carbon to Metal Coating Institute, Queen's University, Kingston, Ontario, K7L 3N6, Canada

Electronic Supplementary Information available. See DOI: 10.1039/x0xx00000x





Scheme 1. Schematic representation of the interaction of N-heterocyclic carbene (NHC) with Cu powder surface resulting in oxide reduction and concurrent formation of a stable NHC film on Cu powder for thermal spray applications.

Organic ligands called N-heterocyclic carbenes (NHCs) have recently been reported to reduce and subsequently functionalize planar copper oxide surfaces.²³⁻²⁶ NHCs have been shown to interact strongly with a plethora of other metal surfaces including gold,^{24, 26-28} magnesium,²⁹ platinum,³⁰ silver,²⁶ ruthenium, and cobalt.³¹ The resulting NHC-based self-assembled monolayers (SAMs) have been proven to be stable in a range of extreme conditions.^{23, 27} While thiol-based SAMs have also been studied for their capability to remove surface oxide followed by the formation of a self-assembled monolayer (SAM) on Cu surfaces,³²⁻³⁴ thiol-based analogs of SAMs are not stable under ambient conditions, especially on reactive surfaces such as Cu,^{35, 36} thus limiting their applications for ambient and aqueous conditions.

Herein, the ability of a common NHC precursor, 1,3-diisopropyl benzimidazolium hydrogen carbonate (NHC•H₂CO₃) to remove surface oxide from copper powder, stabilize the resulting reduced Cu powder, and be employed on scales appropriate for HVOF experiments is described. The mechanical and corrosion properties of the resulting Cu-sprayed coatings were characterized and demonstrated the potential of carbene chemistry in producing corrosion-resistant Cu-sprayed coatings. Finally, the life cycle assessment (LCA) approach as standardized by ISO (2006)^{37, 38} was employed to evaluate a one-pot immersion method for creating stable NHC films on Cu powder. As part of a responsible research and innovation process, the goal of the LCA study is to assess the environmental implications of this methodology in the research and development phase, to identify potential environmental hotspots, and to develop a more sustainable process.

Results and Discussion

View Article Online

DOI: 10.1039/D4TA07631A

NHC Functionalization on Cu Powder Surface

The powder was immersed in a 10 mM NHC•H₂CO₃ solution (Scheme 1) in MeOH with stirring for 24 h. Once Cu powder settled at the bottom of the flask, the supernatant solution was removed followed by triturating the powder 3-4 times with MeOH. The NHC•H₂CO₃ functionalizes the Cu powder surface in two steps. In the first step, free carbene is generated from NHC•H₂CO₃ in MeOH, releasing water and carbon dioxide (Scheme 1).^{23, 39} The generated free carbene reacts with oxidized Cu surfaces to remove Cu surface oxide. In the second step, the freshly exposed Cu metal reacts with the excess NHC in the solution to form a thin protective layer on the Cu surface preventing its re-oxidation. Electrospray ionization-mass spectrometry (ESI-MS) (Figure S26) was conducted on the aliquot solution to provide insight into the mechanism of this process. This technique confirms the presence of oxidized NHC fragments at masses 219 (cyclic urea) and 221 (aldehyde) (the structure of fragments is presented in Figure S26). It confirms that the free carbene successfully interacts with the oxidized Cu surface, reducing the Cu surface (also proved later by XPS) and simultaneously producing oxidized carbene species. The proposed mechanism is consistent with previous literature studies by Veinot et al.²³ and Selva et al.³⁹ on-copper surfaces. After treatment, the Cu particles maintain their spheroidal structure (SEM Figure 1A-B). The particle size distribution (PSD) assessed via dynamic light scattering (DLS) shows no significant disintegration or agglomeration with Dv(50) values of 12.1 μm and 15.2 μm for untreated-Cu and NHC-treated Cu powder, respectively (Table S3, and Figure S2). The immersion treatment preserves powder morphology under tested conditions, which is crucial for thermal spray applications.^{13, 14, 40-42}

The presence of an NHC film on the Cu powder was assessed by X-ray photoelectron spectroscopy (XPS) and laser desorption/ionization-time of flight spectroscopy (LDI-ToF). XPS survey spectra were acquired for untreated-Cu and NHC-treated Cu powders (Figure S5), showing the presence of expected elements (O, C, N, and Cu). The survey scan analysis confirms the powder purity, with no contaminants observed other than trace amounts of Na and Pb. The atomic ratios of O:C:N were 38:36:2 for NHC-treated Cu powder vs. 41:34:0.1 for untreated-Cu powder showing a minor change in the O:C ratio and an increase in the N content suggesting the presence of NHC on the Cu powder surface after treatment. High-resolution N 1s spectra (Figure 1C) show a small signal at a binding energy of 400 eV in the untreated-Cu sample that may be attributed to environmental N₂ interference or sub-surface nitrogen²³. However, this signal is more significant in NHC-treated Cu samples. To provide more detailed information regarding the source of N on the surface, the LDI-ToF analysis was employed which enables the observation of intact NHC molecules on the surface. This technique showed the presence of NHC species on the surfaces as [NHC]⁺ at the expected m/z ratio of 203.⁴³ No such peak was observed in the untreated-Cu powder (Figure S6).



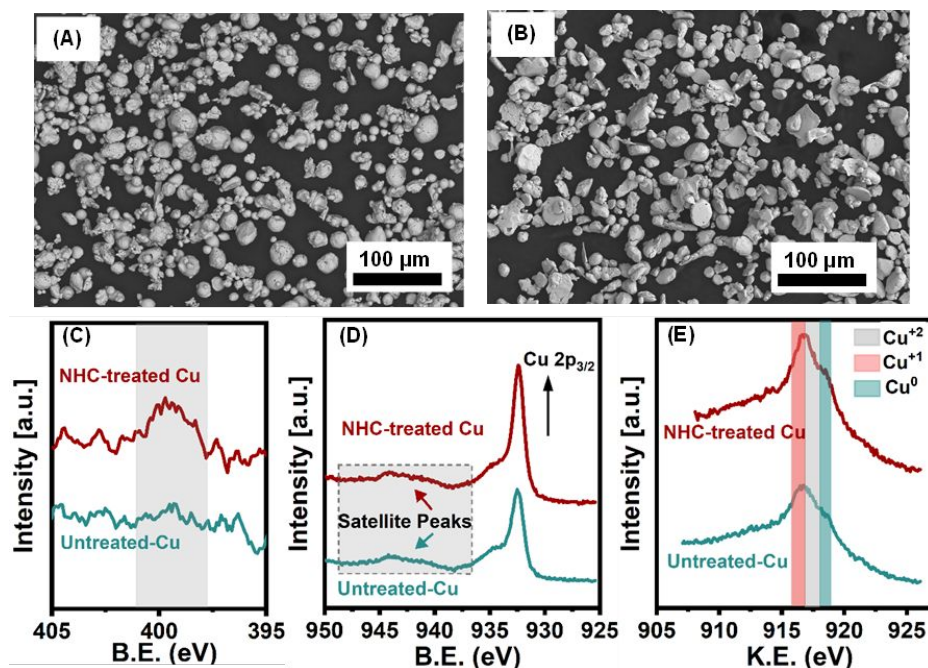


Figure 1. Microscopic images and spectroscopic measurements performed before and after NHC treatment on Cu powder (A) and (B) SEM images of untreated-Cu powder vs. NHC-treated Cu powder showing no significant disintegration; (C), (D) and (E) N 1s, Cu2p_{3/2} and Cu LMM and XPS spectra of untreated-Cu (teal) and NHC-treated Cu (red) powder system showing origin of nitrogen signal after treatment confirming NHC presence and the reduction in Cu (II) species.

These comparative measurements demonstrate the successful functionalization of NHC on Cu powder surface under immersion conditions.

Quantitative insight into the surface oxide removal was next carried out using XPS, which provided high-resolution Cu 2p and Cu LMM Auger spectra. The Cu 2p spectra have a main emission line at 932.5 eV attributed to Cu 2p_{3/2} which has contributions from Cu (0), Cu (I), and Cu (II), present in untreated-Cu and NHC-treated Cu samples. The shake-up satellite peaks⁴⁴ between binding energies of 938 eV and 946 eV are attributed only to Cu (II) species (oxides and hydroxides) and therefore confirm the presence of Cu (II) in untreated-Cu powder samples (Figure 1D, spectra in teal color). The NHC-treated Cu powder has a suppressed shake-up satellite peak due to Cu (II) reduction (Figure 1D, spectra in red) consistent with the previously reported work by the Crudden group on Cu polycrystalline surfaces.²³ From the fitting of the Cu 2p signals, the amount of Cu (II) present using the area under the satellite peaks and a combined Cu (0) + Cu (I) can be calculated (details in experimental 1.6c section, SI).^{45, 46} The amount of Cu (II) species calculated to be present on untreated-Cu and NHC-treated Cu were 43% and 31% respectively (Figure S7A-C, SI) reflecting successful oxide reduction by NHC treatment.

The binding energies for Cu (I) and Cu (0) overlap in Cu 2p spectra making it important to analyze the Cu LMM spectra from the Auger region since peaks for Cu(0), Cu(I), and Cu(II) are present at different kinetic energies (K.E.) in these spectra.^{45, 47} An intense peak for Cu (0) at 918.8 eV K.E. and a reduction in the intensity of Cu (II) peak at 917.7 eV K.E. were observed for the NHC-treated Cu powder, which is consistent with an increase in metallic species and a decrease in Cu (II) species (Figure 1E). The Cu LMM Auger peak fittings showed a

decrease in Cu (II) species by 10% consistent with Cu 2p fittings and an increase in metallic Cu from 7% to 21% after NHC treatment, based on the average of two independent sets of measurements (Figure S7D-F, SI). Thus, surface oxide reduction occurs reliably and reproducibly after the NHC treatment. It should be noted that these reactions and analyses were conducted under ambient conditions, so some re-oxidation in the environment is expected.

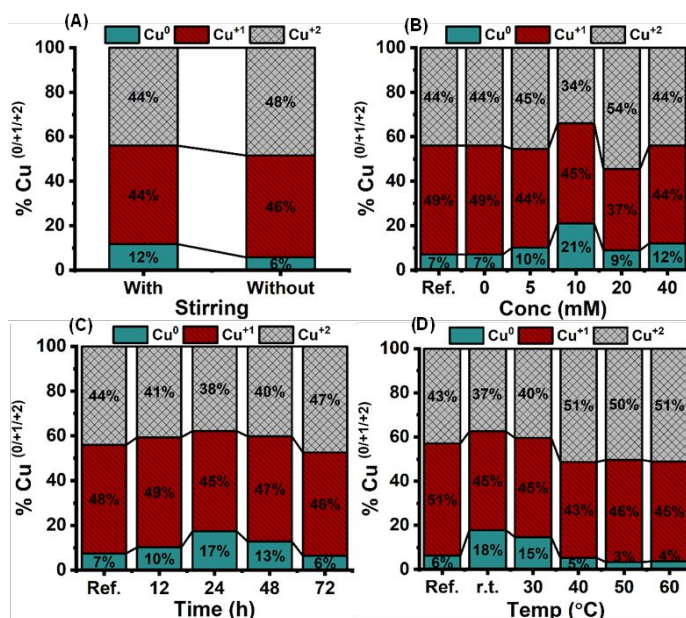
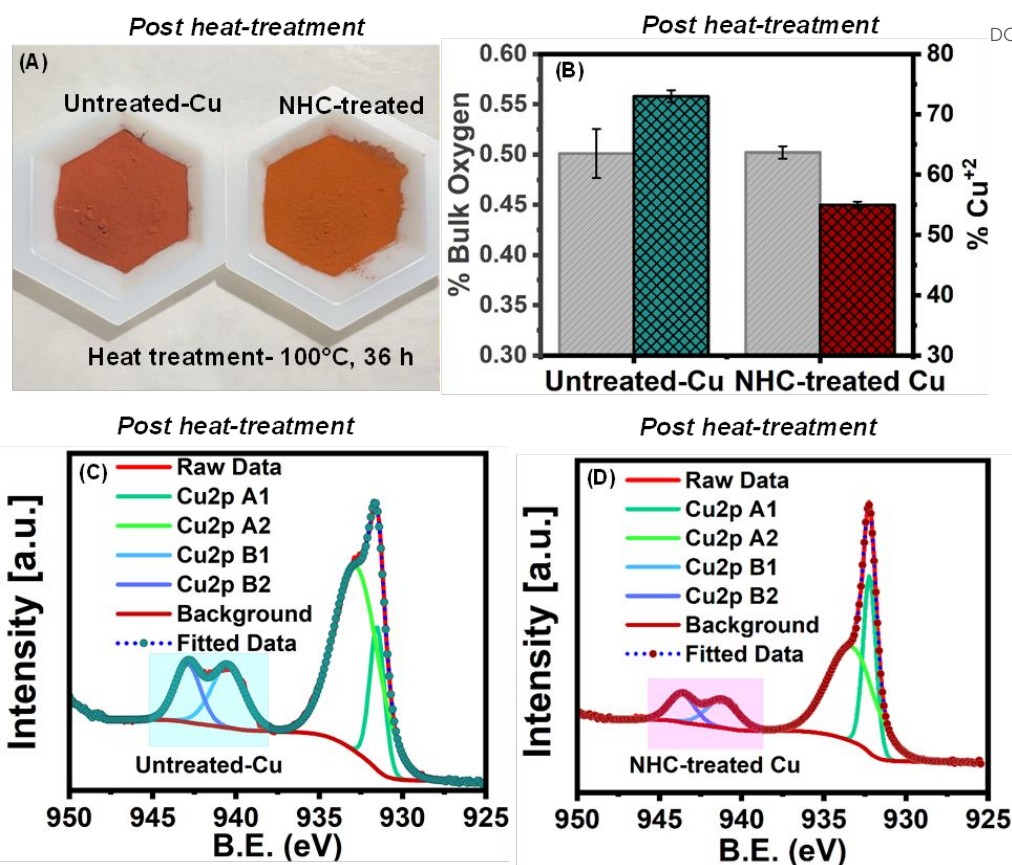


Figure 2. Optimization of NHC film on Cu surface and influence on % of Cu species (0/I/II). The Cu LMM Auger fitting results are presented in a bar graph for (A) Stirring (B) NHC concentration (C) Time of immobilization (D) Effect of temperature, where Ref. stands for reference sample and r.t. stands for room temperature.





ARTICLE

Figure 3. Thermal stability tests to evaluate oxidation resistance of untreated-Cu vs. NHC-treated Cu powder (A) Observation in color change post heat treatment (B) Bar graph presenting % bulk oxygen using ONH elemental analysis using inert fusion technique (Grey) and surface oxygen measurements using XPS (teal for untreated-Cu and red for NHC-treated Cu powder) (C-D) Cu 2p XPS spectra deconvolution for untreated-Cu (teal) vs. NHC-treated Cu powder (red).

Before scale-up, NHC film deposition conditions were optimized in terms of (1) stirring, (2) NHC concentration, (3) immobilization time, and (4) temperature (section 1.3 and 2.2 SI, Figure S8 to S19). The Cu LMM Auger spectra fitting was used as a measure of the amount of Cu in different oxidation states (Figure 2). Optimal conditions were found to be 10 mM NHC concentration and 24 h immersion at room temperature under stirring, which leads to a maximum reduction of Cu (II) species without altering the particle's morphology.

Using these optimized conditions, the chemical stability of NHC-treated vs. untreated-Cu powders was assessed before scale-up and thermal spray. Chemical stability tests were conducted in 0.1M HCl and 0.1M NaOH solutions. The NHC-treated Cu powder was immersed in each solution for 5h, and the LDI-ToF mass spectra (Figure S20) showed the presence of NHC at 203 m/z even after immersion, indicating a strong Cu-NHC bond and a stable film. Additionally, the Cu powder samples were heated at 100 °C for 36 h in an oxygen-rich environment to test their oxidative stabilities. Under these conditions, the untreated-Cu powder turned brown, while the NHC-treated Cu powder showed no significant change in color, suggesting considerable oxidation resistance at high temperatures under an oxygen-rich environment.¹⁴ Post heat-treatment, bulk oxygen measurements were carried out using the ONH elemental analysis (Figure 3B, grey color) by inert gas fusion technique, showing a similar amount of bulk oxygen in untreated-Cu powder vs. NHC-treated Cu powder, with larger errors for the untreated system. Information regarding surface localized copper oxides was obtained using XPS, revealing a significantly higher shake-up peak area in the Cu 2p spectra of untreated-Cu compared to NHC-treated Cu powder. This confirms the higher oxidation resistance of NHC-treated samples (Figure 3C and 3D).

Characterization of Thermally Sprayed Cu Coatings

To produce thermal spray coatings using the untreated-Cu and NHC-treated Cu powder, a thermal spray process using an i7 inner diameter (ID) HVOF gun (Figure S1, SI), with propylene as fuel was employed, with operational parameters summarized in Table S2. A schematic representation of the thermal spraying process, detailing key components of the HVOF gun and coating events can be found in Figure 4B (further details are provided in SI, in the experimental section 1.4 a-c). Thermogravimetric analysis (TGA) was conducted (Figure S25) to understand the

evolution of NHC during thermal spraying and its influence on coating composition post-spraying (Table S5).



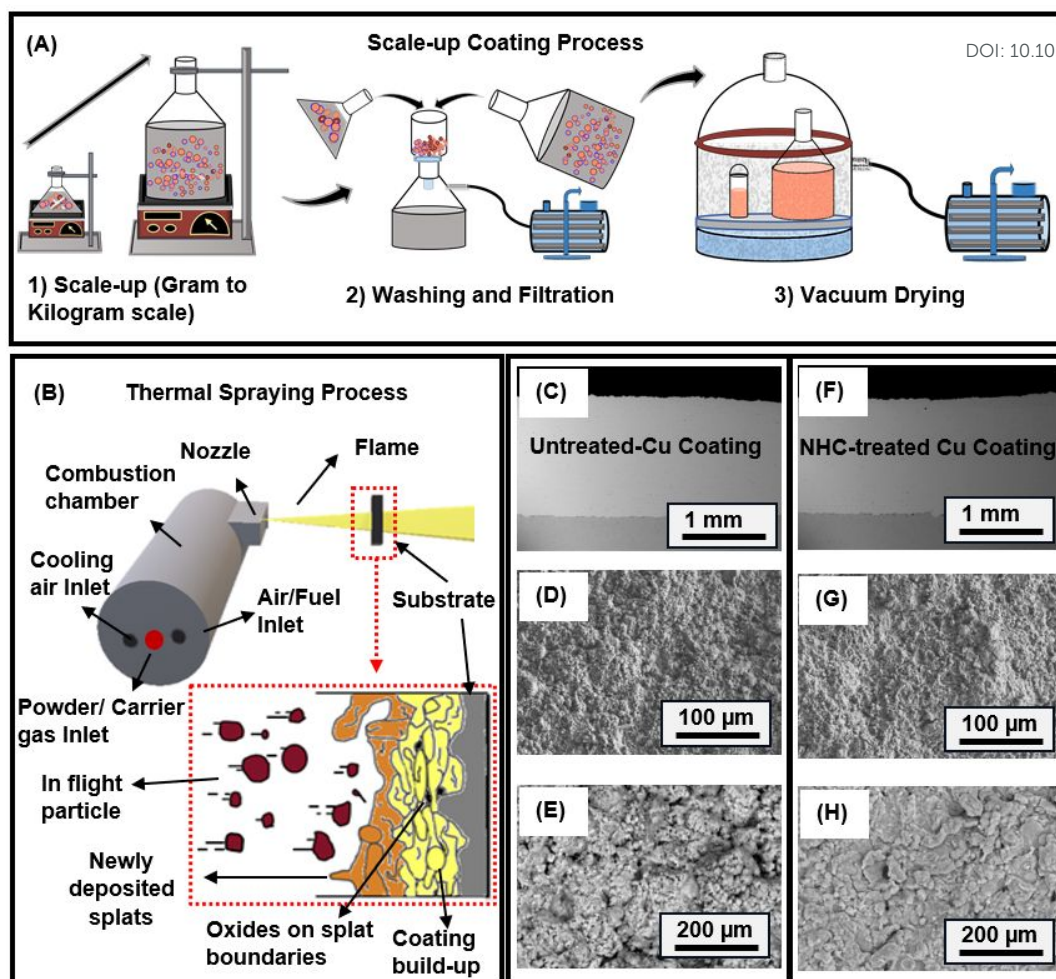


Figure 4. (A-B) Schematic representation of scaling-up for NHC-treated Cu powder and depiction of the thermal spraying process. Microstructure analysis (top view and cross-section view) using SEM for coating build-up using thermal spraying from (C-E) Untreated-Cu and (F-H) NHC-treated Cu powder.

The extensive coating build-up process required at least 1.5 kg powder, requiring the scale-up of the synthetic protocol for the production of the NHC precursor (Figure 4A, precaution; see in experimental section in S.I.). Quality control for this scaled-up procedure was confirmed by the presence of the NHC peak at 203 m/z in the LDI mass spectrum (Figure S21A) and the reduction in surface oxide using XPS, demonstrating that the optimized immersion conditions are also effective at the kilogram scale (Figure S21 B-F). The Cu powder was loaded in the spray gun for thermal spraying on carbon steel surfaces to achieve the Cu-sprayed coatings using untreated-Cu and NHC-treated Cu powder. Deposition efficiencies were 60% and 56% respectively^{22, 48} (calculated using equation S1), showing similar spraying efficacy. Post-spraying, the bulk and surface oxygen content of the coatings was evaluated using ONH elemental analysis and XPS (Figure S24) and O % atomic is presented in table S4.

The microstructural, mechanical, and corrosion properties of the resulting coatings were investigated using SEM, electron backscatter diffraction studies (EBSD), scratch tests, and electrochemical impedance (EIS) measurements. SEM cross-section analysis of thermally sprayed coatings reveals uniform, dense coatings with an average thickness of 1.64 mm

(untreated-Cu powder- Figure 4C) and 1.60 mm (NHC-treated Cu Powder- Figure 4D). Coatings generated from the NHC-treated powder (Figure 4G and 4H) showed smoother microstructural features compared with untreated-Cu powder (Figure 4D and 4E), which indicates better particle deformation under identical spraying conditions, therefore an improved coating.

The crystallographic orientation of the thermal sprayed coatings prepared from NHC-treated Cu powder is characterized using EBSD. It shows more nano-structural well-defined grain boundaries (Figure 5B) in contrast to coatings from untreated-Cu (Figure 5A) and the EBSD phase maps are presented in Figure 5A and 5B insets showing two distinct phases, Cu in red and oxide in black (detailed explanation in section 2.5 SI). This reflects a denser packing and improved adhesion to the carbon steel substrate for NHC-treated copper powder. The cross-section of NHC-treated Cu powder before spraying shows well-defined boundaries (Figure S22) indicating that nano-structural features were formed during immersion treatment, not during the thermal spraying process. The NHC plays a crucial role in removing the surface oxide present on the Cu powder and preventing oxidation of the reduced powders,



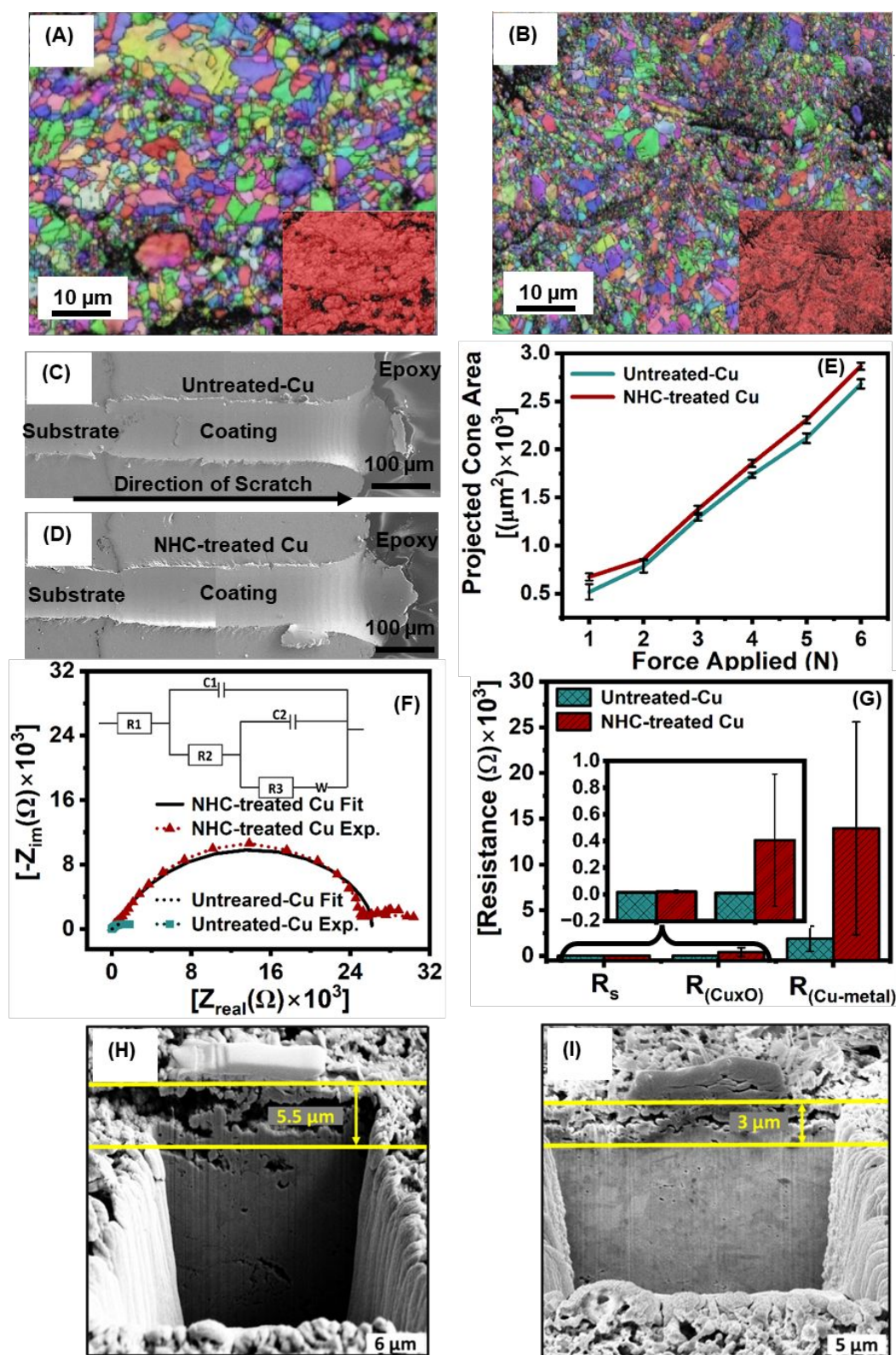


Figure 5. Mechanical and electrochemical characterization of thermally sprayed coatings generated from untreated-Cu and NHC-treated Cu powder surfaces. EBSD measurements show different nano structural grain boundaries of thermally sprayed coatings (A) Untreated-Cu and (B) NHC-treated Cu powder over carbon steel surfaces. The EBSD phase maps are presented in Figure 5A and 5B insets showing two distinct phases, Cu in red and oxide in black (C-D) SEM images were acquired after a scratch test at a 6N load of thermally sprayed coatings from untreated-Cu and NHC-treated Cu powder respectively. (E) Correlation between applied load during the scratch tests and projected cone area collected from SEM images for both kinds of surfaces. (F) Nyquist plot resulting from electrochemical impedance spectroscopic (EIS) investigations on both (A) & (B) surfaces represented by teal and red trace respectively, when measured in a corroding aqueous 3.5% NaCl solution at their respective open circuit potential. The inset in (F) shows the EC-circuit used to fit the EIS data. (G) Average resistance values obtained from multiple measurements as depicted in (F). Post-corrosion FIB-SEM acquisitions are shown in (H) & (I) for (A) and (B) sample surfaces respectively, showing ion penetration (thickness of the corroded area) depth being greater for untreated-Cu powder vs. NHC-treated Cu powder sprayed thermally i.e., more corrosion resistance is offered by the latter surface.

resulting in strong inter-particle bonding and improved coatings.^{9, 13, 14}

The adhesion and cohesion characteristics of untreated-Cu (**Figure 5C**) and NHC-treated Cu (**Figure 5D**) powder coatings were examined using scratch tests on the sample cross-sections.⁴⁹⁻⁵² The test may identify two types of failure: adhesive failure at the interface between the substrate and the coating, and cohesive failure within the coating itself. Coatings were subjected to loads ranging from 1 to 6 N, revealing no adhesive failure. Cohesive failure was assessed via the cone-shaped fracture created by the indenter, which relates the cone area with the cohesive failure (detailed explanation: **section 1.6f SI**). The projected cone area (A_{cn}) was calculated using optical microscope images. No significant difference was observed in A_{cn} for both coatings, suggesting similar cohesive strength in both cases (**Figure 5E**). The untreated-Cu powder sprayed coating displayed brittle areas along the scratch track, whereas the NHC-treated Cu powder sprayed coating showed material removal, suggesting a softer microstructure. No cracks or delamination were observed in either coating, indicating overall robustness.

The characteristics of inter-particle bonding and resulting corrosion resistance were evaluated by performing corrosion tests consisting of electrochemical testing followed by microscopic measurements on untreated-Cu and NHC-treated Cu powder sprayed coatings. Before corrosion testing, all coupons were polished using different grades (800, 1200, and 4000) of SiC paper to remove the thick layer of oxide formed during or after the thermal spray process (**Figure S23**). As shown in **Figure 5F**, the bigger semicircle in the Nyquist plot for the NHC-treated indicates higher corrosion resistance of the sample towards corrosive media vs. untreated-Cu powder sprayed coating. The electrochemical circuit shown in **Figure 5F** (inset) was used to fit the obtained data, which is composed of three resistances, R_1 (solution resistance), R_2 (oxide present on Cu surface), and R_3 (the actual charge transfer resistance offered by the Cu-metal).

As can be seen, a higher charge transfer resistance (R_{CT}) of 13955 Ω (avg of 15 measurements) was observed for the NHC-treated Cu compared to the untreated-Cu (1870 Ω) sprayed surface (**Figure 5G**). The higher charge transfer resistance could be explained based on better inter-particle bonding due to the reduced oxide layer for the NHC-treated Cu thermally sprayed surface. This interpretation is supported by focused ion beam and scanning electron microscope (FIB-SEM) experiments to selectively etch the corroded surface (post-corrosion) for both untreated-Cu (**Figure 5H**) and NHC-treated Cu powder (**Figure 5I**) sprayed coatings. In this experiment, lower penetration of ions was observed for the sprayed coatings from NHC-treated Cu powder. This is also supported by the studies reported by Li et. al.²²

Life Cycle Assessment of the NHC Treatment Process on Cu Powder

Next, the life cycle assessment (LCA) was carried out to evaluate the potential environmental impacts of the immersion method to functionalize Cu powder with NHC and its deposition on steel via the thermal spray application process (HVAF) and identify improvement opportunities. LCA provides a systematic methodology for quantifying environmental burdens associated with products, processes, and systems throughout their life cycle, encompassing stages from raw material acquisition to end-of-life management.⁵³

The preliminary LCA of the environmental footprint associated with NHC-treated Cu powder immersion treatment and the HVAF application process in **Figure 6** is carried out within the context of Quebec (Canada) (**section 1.5 SI** for more details). The process's contribution to climate change is expressed in **Figure 6A** as equivalent kilograms of carbon dioxide (CO_2) and releases an equivalent of 18.5 kg CO_2 -eq. This unit facilitates a comparison of the warming effect of various greenhouse gases to CO_2 , a common reference point.⁵⁴ This analysis shows that the main contributor to the carbon footprint is the production and combustion of propylene for thermal spray. The potential health risks (carcinogenic and non-carcinogenic toxic effects) associated with emitted substances are shown in **Figure 6B** and are compared to a reference chemical, 1,4-dichlorobenzene (1,4-DCB).⁵⁵ The immersion method possesses a potential impact equivalent to 80 kg of 1,4-DCB-eq. While the specific NHC used does not appear to be inherently toxic, Cu within the input materials value chains contributes to overall toxic pollutant emissions.⁵⁶ The third assessment was done to understand the impact of the process on the depletion of non-renewable mineral resources. This assessment converts the mass of all used minerals to an equivalent amount of Cu as a reference element due to its widespread industrial use⁵⁷ and **Figure 6C** (0.23 Cu-eq) indicates the reliance on finite resources in this process.

This holistic approach helps identify improvement opportunities across the product value chain. For instance, adding NHC to Cu powder increases environmental impacts as shown in **Figure 6**, but if it leads to a higher lifetime for the coated material, net environmental benefits could occur. The use phase will be added to this LCA model when data on the performance of the coating will be made available. This will allow for a more complete evaluation of the coating's net environmental benefits, considering the potential trade-off between increased short-term impacts and extended product lifetime.

It is also crucial to note that while the quantity of Cu used significantly exceeds that of carbene, their respective environmental impacts on global warming are comparable. This comparison presents a methodological challenge due to the disparate data sources: industrial-scale data for copper (from the Ecoinvent database) versus a simplified model for carbene synthesis based on laboratory-scale data for the amounts of energy and materials used. It is anticipated that the development of an industrial-scale carbene production process will lead to optimization in reactant usage, energy consumption, and byproduct valorization. Consequently, the LCA results



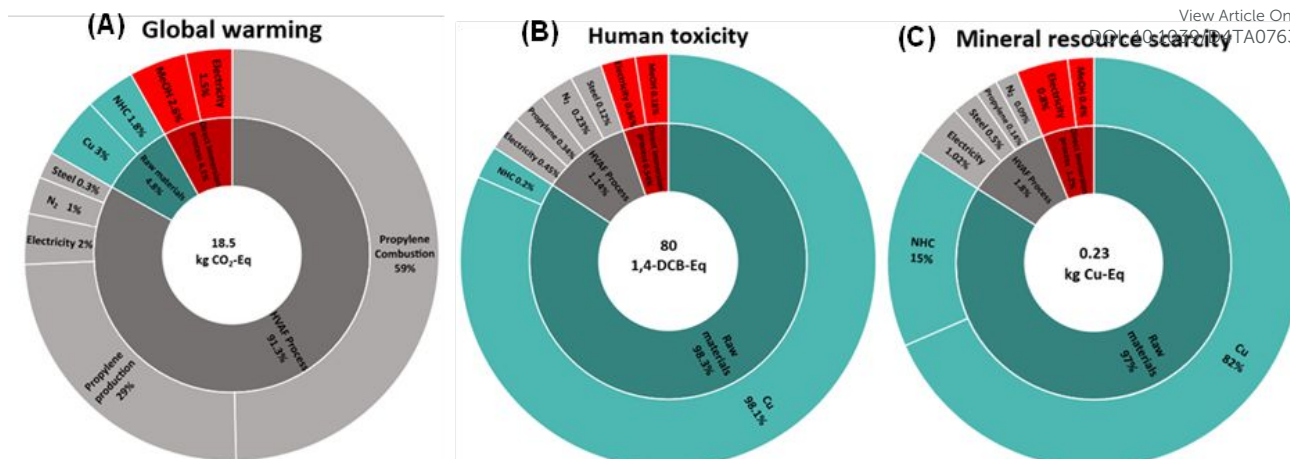


Figure 6. Environmental impact breakdown analysis of the HVAF thermal spraying of 6 samples (32.7 cm² each) of steel using a total of 470g of Cu powder treated with NHC using the immersion method. The pie chart details the primary environmental impact categories, offering a comprehensive overview of the process' implications: (A) global warming impact (kgCO₂-eq), (B) human toxicity potential (kg 1,4-DCB-Eq), and (C) mineral resource scarcity potential (kg Cu-Eq).

obtained are expected to be substantially lower for carbene than the current estimates. An additional factor that can significantly improve environmental performance is using a lower amount of NHC-treated Cu powder for coating build-up using an HVAF gun.

This would reduce the amounts of copper and NHC used, as well as the spray time, which drives the amount of propylene consumed and burned. Although the study focuses on Cu, methanol, and electricity, exploring alternative materials or processes with lower Cu dependence could be valuable for future research.

Conclusions

A reliable, simple, and reproducible one-pot immersion methodology for the reduction of surface oxide and the concurrent formation of an NHC film on Cu powder was successfully developed. The successful surface anchoring of an NHC film on the Cu powder surface was confirmed using XPS and LDI-ToF mass spectroscopy. The maximum increment in metallic features and maximum reduction in surface oxide was observed when 10 mM, 24 h, r.t., and stirring were employed among the examined parameters. Analysis of NHC-treated Cu powder using LDI-ToF mass spectroscopy showed stability of NHC films under extreme pH conditions. XPS analysis confirmed the oxidation resistance of NHC-treated Cu powder vs. untreated-Cu powder at high temperatures under an oxygen-rich environment. The optimized protocol is scalable from gram scale to kilogram scale, with similar film efficiency and reproducibility. HVAF thermal spraying experiments using untreated-Cu and NHC-treated Cu powder produce Cu coatings with thicknesses of approximately 1.6 mm and similar deposition efficiencies. Mechanical strength and corrosion tests were performed after thermal spraying using EBSD, scratch testing, and EIS measurements. Results indicate that thermally sprayed coatings from NHC-treated Cu powder maintain their mechanical properties and show superior corrosion resistance relative to coatings from untreated-Cu powder. The comprehensive LCA study shows potential environmental

impacts and helps to develop more sustainable processes. This study establishes a basis to test the NHC-treated powder using other thermal spray techniques such as cold-spray and compare the properties of generated Cu-sprayed coatings with the HVAF system. The future aim is to test different NHC structures that can further improve inter-particle bonding by reducing more oxide and potentially increasing the lifespan of Cu-sprayed coatings.

Author Contributions

Jashanpreet Kaur – Immersion process, Scale-up process, Stability Tests, XPS including XPS fittings, SEM, DLS measurements, and corresponding evaluation. Wrote, edited, and created Figures for the manuscript.

Golnoush Asadiankouhidehkordi – Thermal Spraying, Stability Test, SEM, DLS, Scratch test, EBSD analysis. Wrote, edited, and created Figures for the manuscript.

Vikram Singh – Assisted in the Scale-up process. EIS and FIB-SEM measurements. Wrote and Edited Manuscript.

Andre C. Liberati – Assisted in the thermal spray process. Edited Manuscript.

Ahmad Diraki - LCA calculations and analysis. Wrote, edited, and created Figures for the manuscript.

Souhaila Bendahmane - LCA calculations and analysis. Wrote, edited, and created Figures for the manuscript.

Mark D. Aloisio – Synthesized NHC.HCO₃. Edited Manuscript.

Payank Patel – Scratch test on Cu-sprayed coatings. Edited Manuscript.

Jeffrey Henderson – Assisted in XPS fittings. Edited Manuscript.

Fadhel Ben Ettouil – Assisted in the thermal spraying process.

Cathleen M. Crudden - Conceptualization, editing, reviewing the manuscript and data analysis/interpretation.

Mark Biesinger - Reviewed XPS fittings and calculations. Edited manuscript.

Annie Levasseur – Reviewed LCA calculations and edited manuscript.



Christian Moreau – Reviewed thermal spray results, conceptualization, supervision, and data analysis/interpretation.

Janine Mauzeroll – Conceptualization, supervision, editing, reviewing the manuscript, and data analysis/interpretation.

Conflicts of interest

The authors declare no conflicts of interest.

Data availability

The data is available on request to the corresponding authors.

Acknowledgments

The authors acknowledge financial support from the NFRF-T Canada (NFRFT-2020-00573). We thank Dr. Nadim Saahe for the kind assistance with LDI-ToF-MS measurements (McGill University). We extend our sincere thanks to the Collaborative Research and Training Experience (CREATE) Excellence in Canadian Corrosion Education through Internationalization, Equity, and Interdisciplinarity (CORRECT) program funded by the Natural Sciences and Engineering Research Council of Canada (NSERC) (CREATE 565232-2022) for providing support to this work. NSERC is also thanked for support through discovery grants to the PIs. The Canada Foundation for Innovation and the Canada Research Chairs programs are thanked for their support. J. Kaur and G. Asadiankouhidehkordi have contributed equally to the paper.

References

- J. R. Davis, *Handbook of thermal spray technology*, ASM international, 2004.
- M. I. Boulos, P. L. Fauchais and J. V. Heberlein, *Thermal spray fundamentals: from powder to part*, Springer, 2021.
- P. L. Fauchais, J. V. Heberlein, M. I. Boulos, P. L. Fauchais, J. V. Heberlein and M. I. Boulos, *Thermal Spray Fundamentals: From Powder to Part*, 2014, 1401-1566.
- T. N. Rhys-Jones, *Surface and Coatings Technology*, 1990, **43**, 402-415.
- G. Asadiankouhidehkordi, A. C. Liberati, F. B. Ettouil and C. Moreau, 2023, 531-537.
- O. Lanz and B. Gries, 2019, 15-22.
- C. Lyphout and S. Björklund, *Journal of Thermal Spray Technology*, 2015, **24**, 235-243.
- S. Wen, C. Dai, W. Mao, Z. Ren, X. Wang, Y. Zhao and G. Han, *Coatings*, 2022, **12**, 458.
- M. Razavipour, S. Rahmati, A. Zúñiga, D. Criado and B. Jodoin, *Journal of Thermal Spray Technology*, 2021, **30**, 304-323.
- T. Stoltenhoff, C. Borchers, F. Gärtner and H. Kreye, *Surface and Coatings Technology*, 2006, **200**, 4947-4960.
- C. L. Nicolaie Markocsan, Lars G. Östergren, Max Sieger.
- N. F. Kazakov, *Diffusion bonding of materials*, Elsevier, 2013.
- C.-J. Li, H.-T. Wang, Q. Zhang, G.-J. Yang, W.-Y. Li and H. Liao, *Journal of Thermal Spray Technology*, 2010, **19**, 95-101.
- X.-T. Luo, Y. Ge, Y. Xie, Y. Wei, R. Huang, N. Ma, C. S. Ramachandran and C.-J. Li, *Journal of Materials Science & Technology*, 2021, **67**, 105-115.
- W.-Y. Li, C.-J. Li and H. Liao, *Applied Surface Science*, 2010, **256**, 4953-4958.
- K. Ko, J. Choi and H. Lee, *Journal of Materials Processing Technology*, 2014, **214**, 1530-1535.
- J. Y. Kim, J. A. Rodriguez, J. C. Hanson, A. I. Frenkel and P. L. Lee, *Journal of the American Chemical Society*, 2003, **125**, 10684-10692.
- P. Kirsch and J. Ekerdt, *Journal of Applied Physics*, 2001, **90**, 4256-4264.
- S. Lee, N. Mettlach, N. Nguyen, Y. Sun and J. White, *Applied Surface Science*, 2003, **206**, 102-109.
- K. Ko, J. Choi, H. Lee and B. Lee, *Powder technology*, 2012, **218**, 119-123.
- K. Chavez and D. Hess, *Journal of The Electrochemical Society*, 2001, **148**, G640.
- Y.-J. Li, X.-T. Luo and C.-J. Li, *Surface and Coatings Technology*, 2021, **407**, 126709.
- A. J. Veinot, A. Al-Rashed, J. D. Padmos, I. Singh, D. S. Lee, M. R. Narouz, P. A. Lummis, C. J. Baddeley, C. M. Crudden and J. H. Horton, *Chemistry - A European Journal*, 2020, **26**, 11431-11434.
- C. R. Larrea, C. J. Baddeley, M. R. Narouz, N. J. Mosey, J. H. Horton and C. M. Crudden, *ChemPhysChem*, 2017, **18**, 3536-3539.
- I. Berg, E. Amit, L. Hale, F. D. Toste and E. Gross, *Angewandte Chemie International Edition*, 2022, 134(25).
- L. Jiang, B. Zhang, A. Paavo Seitsonen, F. Haag, F. Allegretti, J. Reichert, B. Kuster, J. V. Barth and A. C. Papageorgiou, 2017, **8**(12), pp.8301-8308.
- C. M. Crudden, J. H. Horton, I. I. Ebralidze, O. V. Zenkina, A. B. McLean, B. Drevniok, Z. She, H. B. Kraatz, N. J. Mosey, T. Seki, E. C. Keske, J. D. Leake, A. Rousina-Webb and G. Wu, *Nature Chemistry*, 2014, **6**, 409-414.
- A. Krzykawska, M. Wróbel, K. Kozieł and P. Cyganik, *ACS Nano*, 2020, **14**, 6043-6057.
- L. Stephens, J. D. Padmos, M. R. Narouz, A. Al-Rashed, C.-H. Li, N. Payne, M. Zamora, C. M. Crudden, J. Mauzeroll and J. H. Horton, *Journal of The Electrochemical Society*, 2018, **165**, G139.
- Y. Zeng, T. Zhang, M. R. Narouz, C. M. Crudden and P. H. McBreen, *Chemical Communications*, 2018, **54**, 12527-12530.
- J. T. Lomax, E. Goodwin, M. D. Aloisio, A. J. Veinot, I. Singh, W.-T. Shiu, M. Bakiro, J. Bentley, J. F. DeJesus and P. G. Gordon, *Chemistry of Materials*, 2024.
- C. A. Calderon, C. Ojeda, V. A. Macagno, P. Paredes-Oliviera and E. M. Patrio, *The Journal of Physical Chemistry C*, 2010, **114**, 3945-3957.
- D. A. Hutt and C. Liu, *Applied surface science*, 2005, **252**, 400-411.
- M. M. Sung, K. Sung, C. G. Kim, S. S. Lee and Y. Kim, *The Journal of Physical Chemistry B*, 2000, **104**, 2273-2277.
- Y. Wang, J. Im, J. W. Soares, D. M. Steeves and J. E. Whitten, *Langmuir*, 2016, **32**, 3848-3857.
- J. B. Schlenoff, M. Li and H. Ly, *Journal of the American Chemical Society*, 1995, **117**, 12528-12536.



37. I. ISO14040, *Environmental management—life cycle assessment—principles and framework*, 2006, 235-248.
38. I. Standard, *Environmental management-Life cycle assessment-Requirements and guidelines*, ISO, 2006.
39. J. s. SG Selva, Y. Li, J. Kaur, A. Juneau, A. Diraki, S. Bendahmane, J. D. Henderson, M. D. Aloisio, A. Messina and A. Nezamzadeh, *ACS Applied Materials & Interfaces*, 2025.
40. Y.-J. Li, X.-T. Luo and C.-J. Li, *Surface and Coatings Technology*, 2017, **328**, 304-312.
41. J.-T. Liang, S.-F. Chang, C.-H. Wu, S.-H. Chen, C.-W. Tsai, K.-C. Cheng and K. Hsu, *Coatings*, 2023, **13**, 1065.
42. W. Wong, P. Vo, E. Irissou, A. Ryabinin, J.-G. Legoux and S. Yue, *Journal of thermal spray technology*, 2013, **22**, 1140-1153.
43. A. J. Veinot, A. Al-Rashed, J. D. Padmos, I. Singh, D. S. Lee, M. R. Narouz, P. A. Lummis, C. J. Baddeley, C. M. Crudden and J. H. Horton, *Chemistry-A European Journal Supporting Information N-Heterocyclic Carbenes Reduce and Functionalize Copper Oxide Surfaces in One Pot*.
44. J. F. Watts and J. Wolstenholme, *An introduction to surface analysis by XPS and AES*, John Wiley & Sons, 2019.
45. M. C. Biesinger, *Surface and Interface Analysis*, 2017, **49**, 1325-1334.
46. M. C. Biesinger, B. R. Hart, R. Polack, B. A. Kobe and R. S. C. Smart, *Minerals Engineering*, 2007, **20**, 152-162.
47. J. Chastain and R. C. King Jr, *Perkin-Elmer Corporation*, 1992, **40**, 221.
48. Y. Li, Y. Wei, X. Luo, C. Li and N. Ma, *Journal of Materials Science & Technology*, 2020, **40**, 185-195.
49. J. Nohava, B. Bonferroni, G. Bolelli and L. Lusvarghi, *Surface and Coatings Technology*, 2010, **205**, 1127-1131.
50. P. Patel, V. N. V. Munagala, N. Sharifi, A. Roy, S. A. Alidokht, M. Harfouche, M. Makowiec, P. Stoyanov, R. R. Chromik and C. Moreau, *Journal of Materials Science*, 2024, **59**, 4293-4323.
51. C. Sha, Z. Zhou, Z. Xie and P. Munroe, *Surface and Coatings Technology*, 2019, **367**, 30-40.
52. C. Sha, *Chuhan Sha School of Materials Science and Engineering*, 2020.
53. M. A. Curran, *Overview of goal and scope definition in life cycle assessment*, Springer, 2017.
54. P. Forster, T. Storelvmo, K. Armour, W. Collins, J.-L. Dufresne, D. Frame, D. Lunt, T. Mauritsen, M. Palmer and M. Watanabe, 2021.
55. T. E. McKone and E. G. Hertwich, *The International Journal of Life Cycle Assessment*, 2001, **6**, 106-109.
56. M. Pohanka, *Bratisl. Lek. Listy*, 2019, **120**, 397-409.
57. A. Beylot, J. Dewulf, T. Greffe, S. Muller and G.-A. Blengini, *The International Journal of Life Cycle Assessment*, 2024, **29**, 890-908.

View Article Online
DOI: 10.1039/D4TA07631A



The data supporting this article have been included as part of the Supplementary Information.
The raw data is available on request to the corresponding authors.

